Journal of Materials Chemistry A

PAPER

Cite this: J. Mater. Chem. A, 2014, 2, 19653

A highly efficient (>6%) $Cd_{1-x}Mn_xSe$ quantum dot sensitized solar cell

Jianjun Tian,*[a] Lili Lv,[a] Chengbin Fei,[b] Yajie Wang,[b] Xiaoguang Liu[a] and Guozhong Cao*[bc]

Received 1st September 2014
Accepted 24th September 2014

DOI: 10.1039/c4ta04534c

www.rsc.org/MaterialsA

Quantum dot sensitized solar cells (QDSCs) have attracted considerable attention recently and become promising candidates for realizing a cost-effective solar cell. The design and synthesis of quantum dots (QDs) for achieving high photoelectric performance is an urgent need imposed on scientists. Here, we have succeeded in designing a QDSC with a high efficiency η of 6.33% based on $Cd_{0.8}Mn_{0.2}Se$ quantum dots by facile chemical bath deposition (CBD). The effects of Mn^{2+} ions on the physical, chemical, and photovoltaic properties of the QDSCs are investigated. The Mn^{2+} ions doped into QDs can increase the light harvesting to produce more excitons. In addition, the Mn^{2+} dopant also raises the conduction band of CdSe, accelerates the electron injection kinetics and reduces the charge recombination, improving the charge transfer and collection. The increase of the efficiencies of light-harvesting, charge-transfer and charge-collection results in the improvement of the quantum efficiency of the solar cells. The power conversion efficiency of the solar cell is increased to 6.33% (V_{oc} = 0.58 V, J_{sc} = 19.15 mA cm^{-2}, and FF = 0.57).

1. Introduction

Developing low-cost and high-performance solar devices for clean energy sources is becoming an increasingly urgent issue imposed on scientists around the world, as conventional photovoltaic devices, namely crystalline silicon (c-Si) solar cells, suffer from high cost of manufacturing and installation. Now the focus is on next generation solar cells with high efficiency at economically viable cost.[1,2] Semiconductor quantum dots (QDs) are drawing great attention as a material for next generation solar cells due to their high absorption coefficient, tunable band gap and multiple exciton generation (MEG) effect.[3–5] So QDs have been used in dye sensitized solar cells (DSSCs) as the photo-sensitizer instead of organic dyes to form quantum dot sensitized solar cells (QDSCs).[6–8] The typical structure of QDSCs is similar to that of DSSCs, which consists of a mesoporous photoanode (TiO_2 film), a sensitizer (QDs), an electrolyte (polysulfide) and a counter electrode (Cu_2S).[9–11] During operation, photons are captured by QDs, yielding electron–hole pairs that are rapidly separated into electrons and holes at the interface between the nanocrystalline TiO_2 and the QDs. The electrons inject into the TiO_2 film and the holes are released by redox couples in the liquid polysulfide electrolyte.[9,12,13]

Improving the power conversion efficiency (η) of QDSCs has always been an overarching concern for all scientists. One of the approaches has been focused on constructing and fabricating nano-structural oxides, such as TiO_2,[4] ZnO[14,15] and SnO_2[16] to harvest more amounts of QDs. On the other hand, many efforts have been concentrated on designing and synthesizing QDs to achieve high photoelectric performance.[17–19] As for colloidal QDs, doping transition metal ions would lead to new materials showing fascinating electronic and photo-physical properties of QDs.[20,21] So the method of introducing doping metal ions into QDs is believed to be an effective method to improve the performance of QDSCs. Recently, a few studies showed that doping of some ions into sulfide QDs, such as Hg^{2+} into PbS,[22] and Mn^{2+} into CdS,[23] could increase the current density and efficiency of the solar cells. Compared with CdS and PbS QDs, CdSe is more attractive owing to its high potential for light harvesting in the visible light region.[24,25] The efficiency of CdSe sensitized QDSCs is much higher than that of sulfide QD sensitized solar cells.[17,26–30] So doping metal ions into CdSe QDs is thought to be a useful way for designing high efficiency solar cells.[31,32] However, there is little research on the doped CdSe for QDSCs due likely to its difficult formation. In a typical process for the fabrication of QDSCs, QDs can be introduced *via* an approach of *in situ* growth directly from the precursor solutions, which includes successive ionic layer absorption and reaction (SILAR)[33] and chemical bath deposition (CBD).[34] The preparation of CdSe QDs by SILAR needs to be carried out under inert conditions or at high temperature. Compared with SILAR, CBD is a relatively simple method to deposit nanoparticle films

[a]Advanced Materials and Technology Institute, University of Science and Technology Beijing, 100083, China. E-mail: tianjianjun@mater.ustb.edu.cn

[b]Beijing Institute of Nanoenergy and Nanosystems, Chinese Academy of Sciences, 100083, China. E-mail: gzcao@u.washington.edu

[c]Department of Materials and Engineering, University of Washington, Seattle, WA 98195-2120, USA

under ambient conditions, which possesses many advantages, such as stable yield, robust adherence, and uniform and good reproducibility. So CBD is believed to be an appropriate approach for depositing doped CdSe QDs. For transition metal ions, Mn^{2+} is the most common dopant for colloidal QDs to improve the photoluminescence (PL) and quantum yield (QY) of QDs.[20] The dopant creates electronic states in the mid-gap region of the QDs, and thus alters the charge separation and recombination. So, it should be advantageous to produce more excitons to enhance the quantum efficiency of the solar cells using a Mn^{2+} dopant.

Here, we have succeeded in designing a high efficiency QDSC based on $Cd_{1-x}Mn_xSe$ quantum dots. It was found that $Cd_{1-x}Mn_xSe$ is difficult to deposit directly on the surface of TiO_2 oxides. For this reason, the modification of TiO_2 with CdS was adopted to improve the adsorption of $Cd_{1-x}Mn_xSe$ to form a photoanode with the structure of TiO_2/CdS/$Cd_{1-x}Mn_xSe$. This investigation revealed that the doping of Mn^{2+} into the CdSe QDs can significantly influence the performances, such as the light-harvesting, charge-transfer and charge-collection capabilities. As a result, the $Cd_{0.8}Mn_{0.2}Se$ sensitized solar cell exhibited a high conversion efficiency of 6.33% under simulated AM 1.5, 100 mW cm^{-2}.

2. Results and discussion

Deposition of $Cd_{1-x}Mn_xSe$ QDs is implemented by the CBD process in a solution containing 0.1 M sodium selenosulphate (Na_2SeSO_3), 0.1 M mixture of cadmium acetate $Cd(CH_2COO)_2$ and manganese acetate $Mn(CH_2COO)_2$, and 0.2 M trisodium salt of nitrilotriacetic acid ($N(CH_2COONa)_3$) at room temperature for 3 hours. During this process, the Mn^{2+} cation substitutes the Cd^{2+} in CdSe forming $Cd_{0.8}Mn_{0.2}Se$ with a Mn to Cd atomic ratio of 8 : 2 in the reaction solution. The valence state of Mn in quantum dots is determined by X-ray photoelectron spectroscopy (XPS) spectra. Fig. 1 displays the XPS spectra of the nanostructured TiO_2 films loaded with $Cd_{0.8}Mn_{0.2}Se$ QDs. The peak deconvolution process clearly shows that the Mn 2p spectrum of the film is composed of two peaks, at 642 eV and 654 eV, indicating the state of Mn^{2+} in QDs. The composition ratios of Mn/Cd in $Cd_{0.8}Mn_{0.2}Se$ QDs are calculated by energy-dispersive X-ray spectroscopy (EDX). The results of EDX are approximate to those of the ratios in the reaction solution.

Fig. 2(a) displays the UV-visible spectral curves of the films loaded with CdSe and $Cd_{0.8}Mn_{0.2}Se$ QDs. The results reveal that the absorbance of the $Cd_{0.8}Mn_{0.2}Se$ QDs is much higher than that of the CdSe QDs. The high absorbance of the photoelectrode might be attributed to: (1) a greater loading amount of QDs; and (2) the effects of Mn^{2+} doped into QDs. As for the reason (1), the presence of Mn^{2+} in the reaction solution might promote the deposition of QDs. However, our experimental results showed that the colour of the films loaded with $Cd_{1-x}Mn_xSe$ QDs becomes lighter gradually with the increase of the x value, indicating that the amount of QDs is not increased evidently with the increasing Mn content in QDs. So the enhanced absorbance of the photoelectrodes mainly results from reason (2) rather than reason (1). In addition, it is also found that the absorption edges of the film loaded with CdMnSe QDs shift towards short wavelength (blue shift), which derives from the increase of the band gap (E_g) accordingly as shown in Fig. 2(b). Typically, dopant elements will create one fixed energy level, not much dependent on the doping level. However, it might be possible to have much more substitution here, which is not possible in conventional doping. According

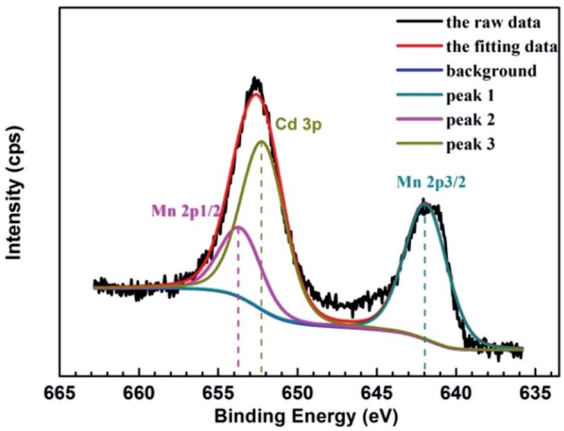

Fig. 1 X-ray photoelectron spectra (XPS) of Mn 2p peaks for Mn doped in CdSe QDs adsorbed on the TiO_2 film.

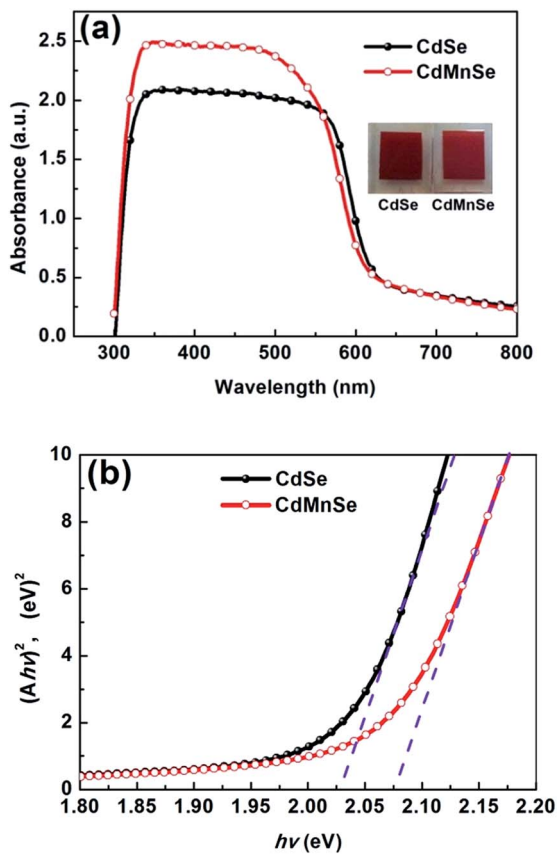

Fig. 2 (a) UV-visible spectral curves and (b) $(Ahv)^2$ *vs.* hv curves of the TiO_2 films loaded with QDs.

to the previous work,[35] the E_g of $Cd_{1-x}Mn_xSe$ QDs is between those of MnSe and CdSe. The increase of E_g is possibly attributed to the high band gap of MnSe (~2.5 eV).[36] In view of the quantum confinement effect, the increase of E_g is attributed to the rise of the conduction band energy (E_{cb}) of QDs to the high energy level.[37] The E_g of QDs can be calculated by plotting $(Ahv)^2$ against the photon energy (hv), where A is the absorbance, h is Plank's constant, and v is the photon frequency.[9,15,27] From Fig. 2(b), the E_g of $Cd_{0.8}Mn_{0.2}Se$ QDs is 2.07 eV, which is higher than the E_g (2.02 eV) of CdSe QDs. According to the band edge alignment of TiO_2/CdS/CdSe (CdMnSe), CdS has a higher E_{cb} than that of CdSe. The Mn dopant could increase the E_{cb} of CdSe, which facilitates the transfer of electrons from QDs to TiO_2.

Fig. 3(a) shows the photoluminescence (PL) spectra of the TiO_2 films loaded with CdSe and $Cd_{0.8}Mn_{0.2}Se$ QDs, respectively. The results reveal that the PL of the film loaded with $Cd_{0.8}Mn_{0.2}Se$ QDs is higher than that of the film loaded with CdSe QDs. The possible reason is attributed to the fact that the Mn^{2+} doped into QDs can cover an emission window similar to that of the current workhorse of intrinsic QDs emitters, leading to the increase of the PL of QDs.[38] The increase of PL also boosts the emission quantum yield (QY) of QDs, which is helpful for producing more excitons. In addition, the dopant creates electronic states in the mid-gap region of the QDs, and thus alters the charge separation and recombination.[20] In a typical PL experiment, a QD is excited with a light-source that provides photons with energy larger than the band-gap energy. Once the photons are absorbed, electrons and holes are formed with finite momenta in the conduction and valence bands, respectively. The emission of photons is derived from the recombination of the electrons and holes. The possible cause of the high PL emission value is that more excitons (electrons and holes) result in more recombination of electrons and holes to emit more photons. However, in the solar cells, the electrons are mainly transferred to electrodes instead of the recombination with holes. So the high PL intensity would boost high charge density in the solar cell. Fig. 3(b) shows the excited state electron radiative decay of the TiO_2 films loaded with CdSe and $Cd_{0.8}Mn_{0.2}Se$ QDs, respectively. The results display that the emission decay of CdMnSe QDs is shorter than that of CdSe QDs, which indicates that the PL lifetime of QDs can be slightly shortened by the Mn^{2+} dopant. The short-lived excited state of the QDs shows the increase of the injection kinetics of photogenerated electrons in the semiconductor.[39] So the Mn^{2+} dopant can accelerate the electron injection from QDs to TiO_2. This result is consistent with the increase in the E_{cb} of CdMnSe QDs facilitating the transfer of electrons from QDs to TiO_2.

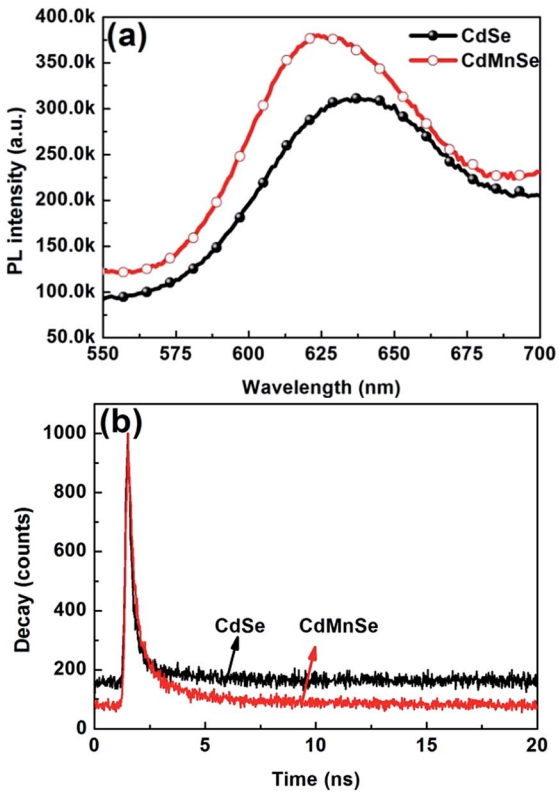

Fig. 3 (a) Photoluminescence (PL) curves (b) excited state electron radiative decay of the TiO_2 films loaded with CdSe and $Cd_{0.8}Mn_{0.2}Se$ QDs, respectively.

Fig. 4(a) displays the impedance spectra of the QDSCs measured under dark conditions with a forward bias of −0.6 V. The fitting results of the impedance spectra are listed in Table 1. In Fig. 4(a), the two semicircles correspond to the electron injection at the counter electrode–electrolyte interface and transport in the electrolyte at high frequencies (R_1), and the electron transfer at the TiO_2/QD/electrolyte interface and transport in the TiO_2 film (R_{ct}), respectively.[40] The R_{ct} is considered as the charge transfer resistance.[41,42] The results show that the value of R_{ct} of the $Cd_{0.8}Mn_{0.2}Se$ sensitized solar cell (39.6 Ω) is much higher than that of the CdSe sensitized solar cell (29.3 Ω). In view of the increase of R_{ct}, the electrons are difficult to recombine with the holes in the electrolyte, which results in the decrease of charge recombination. Although it is very difficult to find out the intrinsic cause of the increase of R_{ct}, we believe the possible reason is that the Mn^{2+} dopant may modify the surface or the interface of QDs to increase the R_{ct} and reduce the charge recombination. Fig. 4(b) shows the Bode plots of the QDSCs with different QDs. The curve peak of the spectrum can be used to determine the electron lifetime according to eqn (1).[43]

$$\tau_n = 1/(2\pi f_{min}) \quad (1)$$

The corresponding results are listed in Table 1, revealing that the electron lifetime of the CdMnSe sensitized solar cell is 89.6 ms, which is twice that of the CdSe sensitized solar cell (41.5 ms). It is clear that the electron lifetime of the solar cell is prolonged by the Mn^{2+} doped into QDs. The electron lifetime (τ_n) is also proportional to R_{ct} and is calculated by eqn (2).[44]

$$\tau_n = R_{ct}C_\mu \quad (2)$$

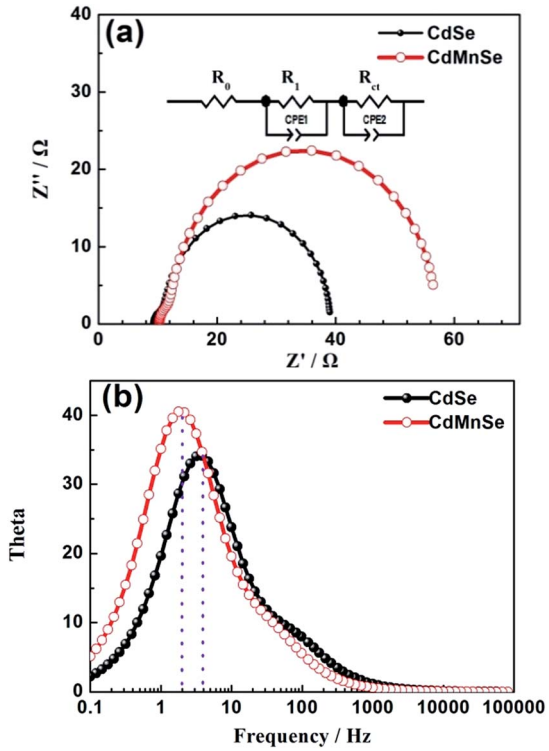

Fig. 4 (a) Nyquist plot and (b) Bode plot curves of the QDSCs under forward bias (−0.6 V) and dark conditions.

where C_μ is the corresponding chemical capacitance. Consequently, the employment of the Mn^{2+} dopant in QDs can enhance the charge recombination resistance and thus prolong the electron lifetime.

It is well known that for the solar cells, electron generation characteristics can be evaluated by the external quantum efficiency (EQE, or incident photon-to-current conversion efficiency, IPCE) and the absorbed photon to current conversion efficiency (APCE). Fig. 5(a) displays the EQE spectra of QDSCs assembled with CdSe and $Cd_{0.8}Mn_{0.2}Se$ QDs, respectively. The maximum EQE of a $Cd_{0.8}Mn_{0.2}Se$ sensitized solar cell reaches 74% at 580 nm, which is enhanced by ~30% compared to the maximum EQE of 58% at 550 nm for a CdSe sensitized one. The EQE is substantially improved from visible to near infrared radiation region 800 nm. The EQE depends on both the absorption of light and the collection of charges. Once a photon has been absorbed and has generated an electron–hole pair, these charges must be separated and collected. The EQE can be estimated by light-harvesting efficiency (LHE), charge-transfer efficiency (η_{ct}), and charge-collection efficiency (η_{cc}), which is expressed by the following equation (eqn (3)).[45]

Table 1 Electrochemical impedance results of QDSCs

Samples	R_1 (Ω)	R_{ct} (Ω)	τ_n (mS)
CdSe	3.2	29.3	41.5
CdMnSe	3.6	39.6	89.6

$$EQE = LHE\eta_{ct}\eta_{cc} \quad (3)$$

The LHE of the solar cell is consistent with the absorbance of the photoelectrode. From the result of the UV-visible spectra (as shown in Fig. 2(a)), the absorbance of $Cd_{0.8}Mn_{0.2}Se$ QDs is much higher than that of CdSe QDs. The high absorbance indicates that a higher LHE can be obtained accordingly. In addition, Fig. 3(a) shows that the increase of PL of CdMnSe QDs can boost the exciton generation due to the improvement of QY. The effect of charge-transfer efficiency (η_{ct}) on EQE spectra is difficult to discuss, because there are not ideal measurements to estimate the efficiency for us. But we could deduce the η_{ct} by the excited state electron radiative decay of QDs, as shown in Fig. 3(b). In view of Fig. 2, the Mn^{2+} dopant could increase the E_{cb} of CdSe, which facilitates the electron transfer to TiO_2. Fig. 3(b) shows that the electron injection from QDs to TiO_2 can be accelerated by the Mn^{2+} dopant. So the increase of E_{cb} and electron injection kinetics is helpful for improving η_{ct}. As for the charge-collection efficiency (η_{cc}), that is mainly contributed by the charge recombination. EIS results (Fig. 4) have revealed that the employment of the Mn^{2+} dopant in QDs can enhance the charge recombination resistance and thus prolong the electron lifetime. Both the drop in the charge recombination and the increase in electron lifetime can cause an enhancement in

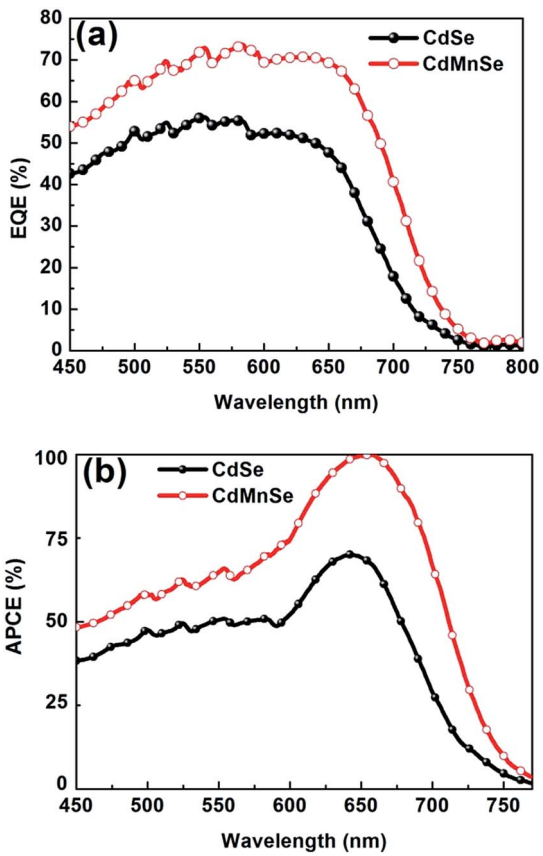

Fig. 5 (a) External quantum efficiency (EQE) spectra curves and (b) absorbed photon to current conversion efficiency (APCE) of QDSCs assembled with CdSe and $Cd_{0.8}Mn_{0.2}Se$ QDs, respectively.

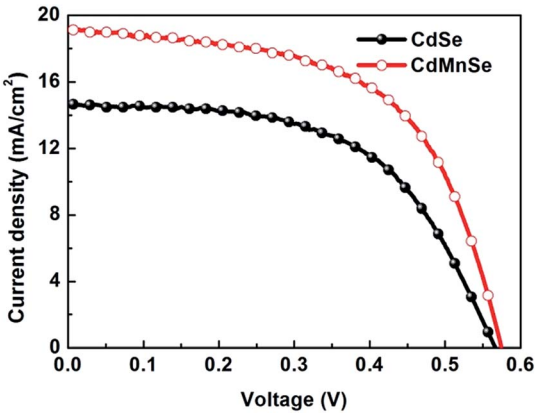

Fig. 6 Photocurrent density–voltage (*J–V*) curves of QDSCs measured under AM 1.5 G, at 1 sun light intensity with a shadow mask.

Table 2 Photovoltaic properties obtained from the *J–V* curves using $Cd_{1-x}Mn_xSe$ QDs as sensitizers

Samples	V_{oc} (V)	J_{sc} (mA cm^{-2})	FF	η (%)
CdSe	0.57	14.65	0.56	4.68 ± 0.22
CdMnSe	0.58	19.15	0.57	6.33 ± 0.35

charge-collection efficiency (η_{cc}). Therefore, it can be deduced that the improved quantum efficiency of the solar cells is ascribed to the increased light-harvesting, charge-transfer and charge-collection efficiencies. Fig. 5(b) shows the APCE spectra of QDSCs assembled with CdSe and $Cd_{0.8}Mn_{0.2}Se$ QDs, respectively. APCE is the absorbed photon to current conversion efficiency and shows how efficiently the absorbed photons are converted into current. It can be seen that the APCE value of the $Cd_{0.8}Mn_{0.2}Se$ sensitized solar cell is much higher than that of the CdSe sensitized solar cell. APCE is obtained by dividing the IPCE number by the light-harvesting efficiency (LHE, 0–100%).[46] So the increase of APCE is mainly attributed to the increase of η_{ct} and η_{cc}.

Fig. 6 shows photocurrent density–voltage (*J–V*) characteristics of the solar cells measured under the illumination of one sun (AM 1.5, 100 mW cm^{-2}). The performance parameters of the solar cells are listed in Table 2. The $Cd_{0.8}Mn_{0.2}Se$ sensitized solar cell exhibits a high performance: J_{sc} = 19.15 mA cm^{-2}, V_{oc} = 0. 58 V, FF = 0.57 and η = 6.33%. It can be seen that the J_{sc} of the solar cell is improved evidently after Mn^{2+} doping, which is the main cause of the improvement of the conversion efficiency. The remarkable increase of J_{sc} is attributed to the excited charge characteristics, such as generation, injection or collection. The Mn^{2+} ions doped into QDs increase the efficiencies of light-harvesting, charge-transfer and charge-collection, which results in the improvement of the EQE of the solar cell resulting in enhanced J_{sc} and η. To the best of our knowledge, the η of 6.33% is one of the highest values for CdSe quantum dot sensitized solar cells at this time.

3. Conclusion

The $Cd_{0.8}Mn_{0.2}Se$ QDs were obtained by facile chemical bath deposition (CBD) and assembled to QDSCs. The Mn^{2+} ions doped into QDs can increase the light harvesting efficiency to produce more excitons. In addition, the Mn^{2+} dopant also raises the conduction band of CdSe, accelerates the exciton injection kinetics and reduces charge recombination, improving the charge transfer and collection. The increase of the efficiencies of light-harvesting, charge-transfer and charge-collection results in the improvement of the external quantum efficiency (EQE) of the solar cells. As a result, $Cd_{0.8}Mn_{0.2}Se$ sensitized solar cells exhibited a high conversion efficiency (η) of 6.33%, which is 30% greater than that of the CdSe sensitized solar cell (4.68%). So the method of doping ions into QDs would be considered as an effective approach to prepare high efficiency QDSCs.

4. Experimental section

TiO_2 film fabrication

TiO_2 mesoporous films with a thickness of 10 ± 0.5 μm were prepared *via* doctor blading on the F:SnO_2 glass (FTO, 8 Ω square^{-1}) substrates using TiO_2 pastes composed of TiO_2 nanoparticles (Degussa P25), ethyl cellulose and α-terpineol.[9] The as-received TiO_2 films were subjected to a sintering process in air at 500 °C for 30 min.

$Cd_{1-x}Mn_xSe$ QD deposition

As a seed layer, CdS QDs were first deposited on the surface of TiO_2 nanoparticles by the successive ionic layer adsorption and reaction (SILAR) method. The detailed experimental procedure could be found in our previous work.[9] And then, $Cd_{1-x}Mn_xSe$ QDs were deposited on the CdS-coated TiO_2 films through a chemical bath deposition (CBD) method. The CdS-coated TiO_2 films were vertically immersed into an aqueous solution containing 0.1 M sodium selenosulphate (Na_2SeSO_3) aqueous solution, 0.1 M mixture of cadmium acetate $Cd(CH_2COO)_2$ and manganese acetate $Mn(CH_2COO)_2$, and 0.2 M trisodium salt of nitrilotriacetic acid ($N(CH_2COONa)_3$) at room temperature for 3 hours. After that, a ZnS passivation layer was deposited by two SILAR cycles while being soaked in an aqueous solution containing 0.1 M zinc nitrate and 0.1 M sodium sulfide, which act as Zn^{2+} and S^{2-} sources, respectively.

Counter electrode and electrolyte

The Cu_2S film was used as the counter electrode in this study, which was prepared on the brass foil as follows: the brass foil was immersed into 37% HCl at 70 °C for 20 min, and then it was washed and dried. The etched brass foil was dipped into aqueous solution containing 1 M S and 1 M Na_2S to form a Cu_2S film. The electrolyte employed in this study was composed of 1 M S and 1 M Na_2S in deionized water.

Materials and QDSC characterization

An FEI Quatan250FEG SEM system equipped with an energy-dispersive X-ray (EDX) spectrometer was employed to estimate the element contents. XPS spectra were collected using an ESCA 2000 spectrometer. The X-ray source was Al Kα and the x axis was fitted for the C 1s peak to have 284.6 eV. The removal of the background signal and integration of the peak was conducted using a VGX900-W system. The absorption spectra were recorded using a Shimadzu UV-3600 spectrophotometer. The photoluminescence (PL) spectra were recorded by using an excitation wavelength of 430 nm at room temperature using a Shimadzu luminescence spectrometer RF-5301PC. The photovoltaic characteristics of the solar cells were evaluated using simulated AM 1.5 sunlight with an output power of 100 mW cm^{-2}. The active area of the QDSCs was 0.1256 cm^2 as determined by a photo-mask. The external quantum efficiency (EQE) spectra were obtained in the range of 400–800 nm using a Keithley 2000 multimeter with illumination using a 300 W tungsten lamp with a Spectral Product DK240 monochromator. The electrochemical impedance spectroscopy (EIS) was carried out with use of an impedance analyzer (ZAHNER CIMPS) under dark conditions at a forward bias of 0.6 V.

Acknowledgements

This work was supported by the National Science Foundation of China (51374029 and 51174247) and the Program for New Century Excellent Talents in University (NCET-13-0668). This work was also supported in part by the National Science Foundation (DMR 1035196), the University of Washington TGIF grant and the Royalty Research Fund (RRF) from the Office of Research at University of Washington and Fundamental Research Funds for the Central Universities (FRF-TP-14-008C1).

Notes and references

1 M. Graetzel, R. A. J. Janssen, D. B. Mitzi and E. H. Sargent, *Nature*, 2012, **488**, 304–312.
2 T. Kinoshita, J. T. Dy, S. Uchida, T. Kubo and H. Segawa, *Nat. Photonics*, 2013, **7**, 535–539.
3 J. Y. Kim, O. Voznyy, D. Zhitomirsky and E. H. Sargent, *Adv. Mater.*, 2013, **25**, 4986–5010.
4 C. Dong, X. Li, X. Fan and J. Qi, *Adv. Energy Mater.*, 2012, **2**, 639–644.
5 J. Tian, Q. Zhang, E. Uchaker, R. Gao, X. Qu, S. Zhang and G. Cao, *Energy Environ. Sci.*, 2013, **6**, 3542.
6 J. H. Bang and P. V. Kamat, *Adv. Funct. Mater.*, 2010, **20**, 1970–1976.
7 V. Gonzalez-Pedro, X. Xu, I. Mora-Sero and J. Bisquert, *ACS Nano*, 2010, **4**, 5783–5790.
8 X.-Y. Yu, J.-Y. Liao, K.-Q. Qiu, D.-B. Kuang and C.-Y. Su, *ACS Nano*, 2011, **5**, 9494–9500.
9 J. J. Tian, R. Gao, Q. F. Zhang, S. G. Zhang, Y. W. Li, J. L. Lan, X. H. Qu and G. Z. Cao, *J. Phys. Chem. C*, 2012, **116**, 18655–18662.
10 T. L. Li, Y. L. Lee and H. Teng, *Energy Environ. Sci.*, 2012, **5**, 5315–5324.
11 T. Sugaya, O. Numakami, R. Oshima, S. Furue, H. Komaki, T. Amano, K. Matsubara, Y. Okano and S. Niki, *Energy Environ. Sci.*, 2012, **5**, 6233–6237.
12 P. V. Kamat, *J. Phys. Chem. C*, 2008, **112**, 18737–18753.
13 P. V. Kamat, *J. Phys. Chem. Lett.*, 2013, **4**, 908–918.
14 J. Tian, Q. Zhang, E. Uchaker, Z. Liang, R. Gao, X. Qu, S. Zhang and G. Cao, *J. Mater. Chem. A*, 2013, **1**, 6770–6775.
15 J. J. Tian, Q. F. Zhang, L. L. Zhang, R. Gao, L. F. Shen, S. G. Zhang, X. H. Qu and G. Z. Cao, *Nanoscale*, 2013, **5**, 936–943.
16 M. A. Hossain, J. R. Jennings, Z. Y. Koh and Q. Wang, *ACS Nano*, 2011, **5**, 3172–3181.
17 Z. X. Pan, H. Zhang, K. Cheng, Y. M. Hou, J. L. Hua and X. H. Zhong, *ACS Nano*, 2012, **6**, 3982–3991.
18 T. Fukumoto, T. Moehl, Y. Niwa, M. K. Nazeeruddin, M. Grätzel and L. Etgar, *Adv. Energy Mater.*, 2013, **3**, 29–33.
19 J.-Y. Jeng, Y.-F. Chiang, M.-H. Lee, S.-R. Peng, T.-F. Guo, P. Chen and T.-C. Wen, *Adv. Mater.*, 2013, **25**, 3727–3732.
20 R. Beaulac, P. I. Archer, S. T. Ochsenbein and D. R. Gamelin, *Adv. Funct. Mater.*, 2008, **18**, 3873–3891.
21 N. S. Karan, D. D. Sarma, R. M. Kadam and N. Pradhan, *J. Phys. Chem. Lett.*, 2010, **1**, 2863–2866.
22 J.-W. Lee, D.-Y. Son, T. K. Ahn, H.-W. Shin, I. Y. Kim, S.-J. Hwang, M. J. Ko, S. Sul, H. Han and N.-G. Park, *Sci. Rep.*, 2013, **3**, 1050.
23 P. K. Santra and P. V. Kamat, *J. Am. Chem. Soc.*, 2012, **134**, 2508–2511.
24 G. Zhu, L. Pan, T. Xu and Z. Sun, *ACS Appl. Mater. Interfaces*, 2011, **3**, 3146–3151.
25 Y. H. Lee, S. H. Im, J. A. Chang, J. H. Lee and S. I. Seok, *Org. Electron.*, 2012, **13**, 975–979.
26 M. A. Hossain, J. R. Jennings, C. Shen, J. H. Pan, Z. Y. Koh, N. Mathews and Q. Wang, *J. Mater. Chem.*, 2012, **22**, 16235–16242.
27 Z. Pan, K. Zhao, J. Wang, H. Zhang, Y. Feng and X. Zhong, *ACS Nano*, 2013, **7**, 5215–5222.
28 J. G. Radich, N. R. Peeples, P. K. Santra and P. V. Kamat, *J. Phys. Chem. C*, 2014, **118**, 16463–16471.
29 J. Wang, I. Mora-Sero, Z. Pan, K. Zhao, H. Zhang, Y. Feng, G. Yang, X. Zhong and J. Bisquert, *J. Am. Chem. Soc.*, 2013, **135**, 15913–15922.
30 K. Yan, L. Zhang, J. Qiu, Y. Qiu, Z. Zhu, J. Wang and S. Yang, *J. Am. Chem. Soc.*, 2013, **135**, 9531–9539.
31 Q. Dai, E. M. Sabio, W. Wang and J. Tang, *Appl. Phys. Lett.*, 2014, **104**, 183901.
32 T. Debnath, P. Maity, S. Maiti and H. N. Ghosh, *J. Phys. Chem. Lett.*, 2014, **5**, 2836–2842.
33 Z. Yang, Q. Zhang, J. Xi, K. Park, X. Xu, Z. Liang and G. Cao, *Sci. Adv. Mater.*, 2012, **4**, 1013–1017.
34 X. Huang, S. Huang, Q. Zhang, X. Guo, D. Li, Y. Luo, Q. Shen, T. Toyoda and Q. Meng, *Chem. Commun.*, 2011, **47**, 2664–2666.
35 L. Yang, R. Zhou, J. Lan, Q. Zhang, G. Cao and J. Zhu, *J. Mater. Chem. A*, 2014, **2**, 3669–3676.

36 S. J. Youn, B. I. Min and A. J. Freeman, *Phys. Status Solidi B*, 2004, **241**, 1411–1414.
37 J. R. I. Lee, R. W. Meulenberg, K. M. Hanif, H. Mattoussi, J. E. Klepeis, L. J. Terminello and T. van Buuren, *Phys. Rev. Lett.*, 2007, **98**, 146803.
38 N. Pradhan and X. Peng, *J. Am. Chem. Soc.*, 2007, **129**, 3339–3347.
39 P. R. F. Barnes, A. Y. Anderson, S. E. Koops, J. R. Durrant and B. C. O'Regan, *J. Phys. Chem. C*, 2009, **113**, 1126–1136.
40 N. Koide, A. Islam, Y. Chiba and L. Y. Han, *J. Photochem. Photobiol., A*, 2006, **182**, 296–305.
41 K. Park, Q. F. Zhang, B. B. Garcia, X. Y. Zhou, Y. H. Jeong and G. Z. Cao, *Adv. Mater.*, 2010, **22**, 2329–2332.
42 K. Park, Q. F. Zhang, B. B. Garcia and G. Z. Cao, *J. Phys. Chem. C*, 2011, **115**, 4927–4934.
43 R. Kern, R. Sastrawan, J. Ferber, R. Stangl and J. Luther, *Electrochim. Acta*, 2002, **47**, 4213–4225.
44 Q. Wang, S. Ito, M. Gratzel, F. Fabregat-Santiago, I. Mora-Sero, J. Bisquert, T. Bessho and H. Imai, *J. Phys. Chem. B*, 2006, **110**, 25210–25221.
45 S. S. Shin, J. S. Kim, J. H. Suk, K. D. Lee, D. W. Kim, J. H. Park, I. S. Cho, K. S. Hong and J. Y. Kim, *ACS Nano*, 2013, **7**, 1027–1035.
46 A. Hagfeldt, G. Boschloo, L. Sun, L. Kloo and H. Pettersson, *Chem. Rev.*, 2010, **110**, 6595–6663.